

## A novel Alcohol Biosensor Based on Alcohol Dehydrogenase and Modified Electrode with ZrO<sub>2</sub> Nanoparticles

Farough Salimi<sup>1</sup>, Masoud Negahdary<sup>2,\*</sup>, Gholamreza Mazaheri<sup>2</sup>, Hajar Akbari-dastjerdi<sup>2</sup>, Yousoof Ghanbari-kakavandi<sup>2</sup>, Sholeh Javadi<sup>2</sup>, Seyed hosein Inanloo<sup>3</sup>, Maryam Mirhashemi-route<sup>3</sup>, Mohammad hani Shokoohnia<sup>3</sup> and Aida Sayad<sup>2</sup>

<sup>1</sup> Kermanshah University of medicine, Kermanshah, Iran

<sup>2</sup> Department of Biology, Payame Noor University, I.R. of IRAN

<sup>3</sup> Department of Restorative, Islamic Azad University, Dental Branch, Tehran, Iran

\*E-mail: [masoud.negahdary@hotmail.com](mailto:masoud.negahdary@hotmail.com)

Received: 5 June 2012 / Accepted: 12 July 2012 / Published: 1 August 2012

---

In this study, we developed an electrochemical ADH-based biosensor as a simple and convenient tool for the detection of ethanol. The carbon paste electrode was modified with ZrO<sub>2</sub> nanoparticles. Direct electrochemistry of ADH in this paste electrode was easily achieved, and a pair of well-defined quasireversible redox peaks appeared with a formal potential ( $E^0$ ) of  $-(450 \pm 1)$  mV (versus SCE) in pH 7.0 phosphate buffer solution (PBS). The linear range of this biosensor for ethanol determination was from 1 to 26 mM. This novel biosensor showed high sensitivity, a wide linear range, low detection limit and good stability for electrochemical detection of ethanol. This work may represent a facile, cheap and promising approach for the fabrication of various electrochemical biosensors.

---

**Keywords:** alcohol biosensor, alcohol dehydrogenase, Zirconia nanoparticles, carbon paste electrode

### 1. INTRODUCTION

Biosensor molecules detect signal using a transducer e.g. optical, electrochemical, piezoelectric and gravimetric transducers are used to get signals in these devices. So the central theme of detection is the signal transduction associated with the selective recognition of a biological or chemical species [1-2]. There are two different types of biosensors: biocatalytic and bioaffinity-based biosensors. The biocatalytic biosensor uses mainly enzymes as the biological compound, catalyzing a signaling biochemical reaction [3]. The bioaffinity based biosensor, designed to monitor the binding event itself, uses specific binding proteins, lectins, receptors, nucleic acids, membranes, whole cells, antibodies or antibody-related substances for biomolecular recognition[4-6]. A chemical biosensor is a sensor that

produces an electric signal proportional to the concentration of biochemical analytes. These biosensors use chemical as well as physical principles in their operation [7-8]. Based on unique physical, chemical and electrocatalytic properties, nanoparticles play variety of roles in different biosensing systems. The attachment of nanoparticles onto electrodes drastically enhances the conductivity and electron transfer from the redox analytes to make them electroanalytical sensor [9]. The control of food quality and freshness is of growing interest for both consumer and food industry. In the food industry, the quality of a product is checked using conventionally techniques as, chromatography, spectrophotometry and others [10]. These methods are expensive, slow, need well trained operators and in some cases, require steps of extraction or sample pretreatment, increasing the time of analysis. The food and drink industries need rapid methods to determine compounds of interest [11-13]. An alternative to facilitate the analysis in routine of industrial products is the biosensors development. The determination of alcoholic compounds, particularly of ethanol, is relevant to the food industry, especially in alcoholic beverages such as beer, wines and spirits [14-15]. In the case of ethanol a number of enzyme-based electrochemical devices have been developed. For this purpose there are two enzymes: alcohol oxidase and alcohol dehydrogenase. The alcohol dehydrogenase is a NADH depending enzyme and the biosensors for ethanol based on this enzyme require the co-immobilization of both enzyme and co-enzyme [16]. To achieve efficient ethanol quantification in clinical, food and beverage industries, alcohol dehydrogenase (ADH) based biosensors have been widely used. ADH catalyzes the oxidation of ethanol to acetaldehyde using nicotinamide adenine dinucleotide ( $\text{NAD}^+$ ) as a cosubstrate [17]. In ADH based ethanol biosensors irreversible oxidation of ethanol occurs in presence of both ADH and its cofactor  $\text{NAD}^+$  at their close proximity [18]. The various immobilization matrices used in the past for ADH immobilization are ferrocene encapsulated ormosils [19], polyethylene glycol [20], colloidal gold [21], conducting polymers [22], redox polymers [23], multi-walled carbon nanotubes composite films and metal oxide nanoparticles [24-26]. Due to special properties of  $\text{ZrO}_2$  nanoparticles we used of this nanoparticle as facilitator [27]. In this work, we designed a novel alcohol biosensor based on alcohol dehydrogenase and modified electrode with  $\text{ZrO}_2$  nanoparticles. This biosensor introduced new and cheap way for detection of alcohols.

## 2. EXPERIMENTAL

### 2.1. Materials

Zirconyl chloride octahydrate purchased from Sigma-Aldrich. Alcohol dehydrogenase (ADH), NADH and  $\text{NAD}^+$  were obtained from Merck and Other Reagents purchased from Merck. The supporting electrolyte used for all experiments is 0.1 M pH 7 phosphate buffer solution (PBS), which is prepared by using 0.1 M  $\text{Na}_2\text{HPO}_4$  and  $\text{NaH}_2\text{PO}_4$  solutions. All the reagents used were of analytical grade and all aqueous solutions were prepared using doubly distilled water.

### 2.2. Apparatus

Cyclic voltammetry (CV) and square wave voltammetry were performed using an Autolab potentiostat PGSTAT 302 (Eco Chemie, Utrecht, The Netherlands) driven by the General purpose

Electrochemical systems data processing software (GPES, software version 4.9, Eco Chemie). A conventional three-electrode cell was employed throughout the experiments, with bare or ZrO<sub>2</sub> nanoparticles modified carbon paste electrode (4.0mm diameter) as a working electrode, a saturated calomel electrode (SCE) as a reference electrode, and a platinum electrode as a counter electrode. The phase characterization of ZrO<sub>2</sub> nanoparticles was performed by means of X-ray diffraction (XRD) using a D/Max-RA diffractometer with CuK $\alpha$  radiation. Surface morphological properties of ZrO<sub>2</sub> nanoparticles were studied by JEM-200CX transmission electron microscopy (TEM).

### 2.3. Preparation of ZrO<sub>2</sub> nanoparticles

The ZrO<sub>2</sub> nanoparticles were prepared according to the literature. Initially, 2.58 g ZrOCl<sub>2</sub>·8H<sub>2</sub>O and 4.80 g urea were dissolved in 20.0 mL CH<sub>3</sub>OH under stirring to form a colorless solution. The solution was transferred to a 20-mL Teflon-lined stainless steel autoclave, which was heated to 200 °C and maintained at that temperature for 20 h. The obtained white product was post-treated with sulphuric acid solution (0.167 mmol), and then calcined at 645 °C.

### 2.4. Preparation of unmodified carbon paste electrode (CPE) and modified CPE with ZrO<sub>2</sub> Nanoparticles

Unmodified carbon paste electrode was prepared by mixing 65% graphite powder and 35% paraffin wax. Paraffin wax was heated till melting and then, mixed very well with graphite powder to produce a homogeneous paste. The resulted paste was then packed into the end of an insulin syringe (i.d.: 2mm). External electrical contact was established by forcing a copper wire down the syringe. CPE modified with zirconia Nanoparticles was prepared by mixing 60% graphite powder and 30% paraffin wax with and 15% zirconia Nanoparticles. The surface of the electrode was polished with a piece of weighting paper and then rinsed with distilled water thoroughly.

## 3. RESULTS AND DISCUSSION

### 3.1. X-Ray diffraction of ZrO<sub>2</sub> nanoparticles

The XRD pattern Fig. 1 for ZrO<sub>2</sub> nanoparticles, the diffraction peaks are absorbed at 2 $\theta$  values. The prominent peaks have been utilized to estimate the grain size of sample with the help of Scherrer equation [28]  $D = K\lambda/(\beta \cos \theta)$  where K is constant(0.9),  $\lambda$  is the wavelength( $\lambda = 1.5418 \text{ \AA}$ ) (Cu K $\alpha$ ),  $\beta$  is the full width at the half-maximum of the line and  $\theta$  is the diffraction angle. The grain size estimated using the relative intensity peak for ZrO<sub>2</sub> nanoparticles was found to be 20 nm and increase in sharpness of XRD peaks indicates that particles are in crystalline nature. All different peaks in figure 1 related to ZrO<sub>2</sub> nanoparticles and matched to Joint Committee for Powder Diffraction Studies.

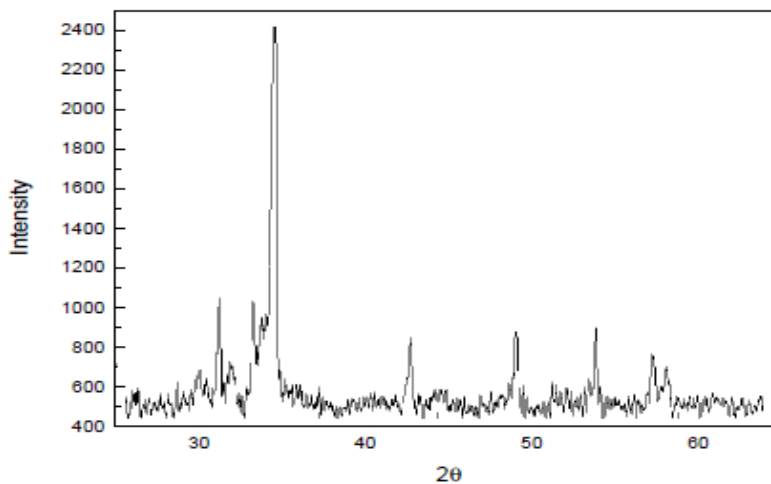


**Figure 1.** XRD pattern for ZrO<sub>2</sub> nanoparticles

3.2. Electron Microscopic Investigation of ZrO<sub>2</sub> Nanoparticles

As it is well known, the properties of a broad range of materials and the performance of a large variety of devices depend strongly on their surface characteristics. Figure 2 (a&b) showed the typical images of ZrO<sub>2</sub> Nanoparticles. Both two part of image were captured at 150 kv with TEM microscopy. The magnification was 150 KX for part (a) of Figure 2, but magnification was 80 KX for part (b) of Figure 2. The average diameter of the synthezsd ZrO<sub>2</sub> nanoparticles is about 20 nm, and has a very narrow particle distribution.

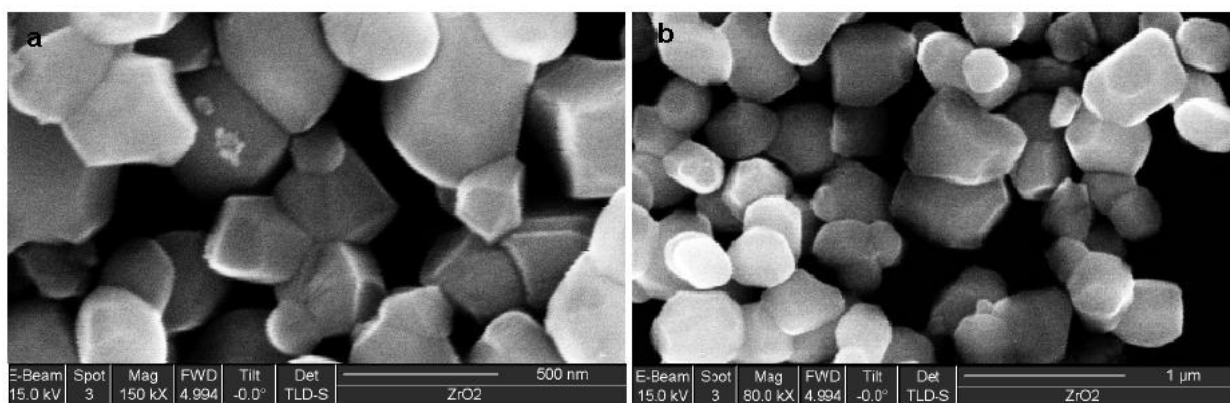


**Figure 2.** TEM image of ZrO<sub>2</sub> nanoparticles (a) captured image size was 500 nm at 150 KX magnification and (b) captured image size was 1 μm at 80 KX magnification.

3.3. Direct electrochemistry of the modified carbon paste electrode with ADH and ZrO<sub>2</sub> nanoparticles

The direct electrochemistry behavior of ADH / ZrO<sub>2</sub> Nps/ CPE was studied as shown in Fig. 3. It can be seen in cyclic voltammograms (Fig. 3 (b) ) that a pair of well-defined redox peaks was observed at the ADH / ZrO<sub>2</sub> Nps/ CPE in a 0.1 mol L<sup>-1</sup> phosphate buffer solution (PBS) of pH 7.0 at a

scan rate of  $50\text{mVs}^{-1}$  compared to the  $\text{ZrO}_2$  Nps/ CPE (Fig. 3 (a) ). Its anodic peak potential and cathodic peak potential were located at  $-400\text{mV}$  and  $-500\text{mV}$  (vs. SCE), respectively. Obviously, these peaks were attributed to the redox reaction of the electroactive probe of Alcohol Dehydrogenase. ADH / CPE also showed the response of alcohol dehydrogenase, but the response was much smaller than that of ADH /  $\text{ZrO}_2$  Nps/ CPE (not shown). Thus, the adsorption of alcohol dehydrogenase and  $\text{ZrO}_2$  nanoparticles on electrode surface played an important role in facilitating the electron exchange between the electroactive center of alcohol dehydrogenase and CPE. The formal potential ( $E^0$ ) of alcohol dehydrogenase, estimated as the midpoint of reduction and oxidation potentials, was  $-(450 \pm 1)\text{mV}$ .

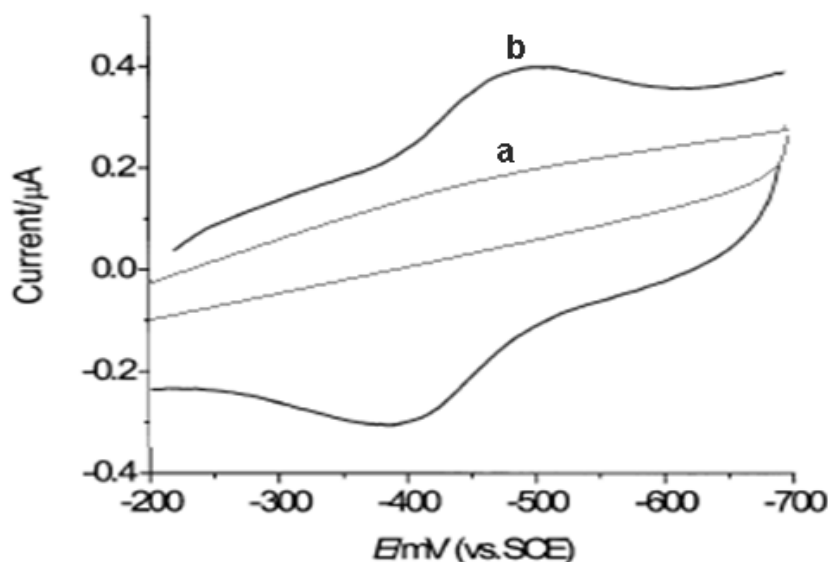


**Figure 3.** Cyclic voltammograms, using (a) the  $\text{ZrO}_2$  NPs/CPE in 0.1 M phosphate buffer and (b) ADH /  $\text{ZrO}_2$  Nps/ CPE in 0.1 M phosphate buffer (scan rate: 50 mV/s).

Fig. 4(a) shows the cyclic voltammograms of the ADH /  $\text{ZrO}_2$  Nps/ CPE in 0.1 mol  $\text{L}^{-1}$  phosphate buffer solution of pH 7.0 at different scan rates (10, 25, 50, 100, 200 and 400  $\text{mV s}^{-1}$ ). The peak currents increased and the cathodic and anodic peak potentials exhibited a small shift along with the increase of scan rate. On the grounds that the surface-to-volume ratio increases with the size decrease and because of the fact that the enzyme size is comparable with the nanometer-scale building blocks, these nanoparticles displayed a great effect on the electron exchange assistance between ADH and carbon paste electrode. For further investigate the ADH characteristics at the ADH /  $\text{ZrO}_2$  Nps/ CPE, the effect of scan rates on the ADH voltammetric behavior was studied in detail. The baseline subtraction procedure for the cyclic voltammograms was obtained in accordance with the method reported by Bard and Faulkner [29]. The scan rate ( $v$ ) and the square root scan rate ( $v^{1/2}$ ) dependence of the heights and potentials of the peaks are plotted in Fig. 4b and c. It can be seen that the redox peak currents increased linearly with the scan rate, the correlation coefficient was 0.9818 ( $i_{pc} = 0.0038v + 0.2302$ ) and 0.9735 ( $i_{pa} = -0.0041v - 0.1152$ ), respectively. This phenomenon suggested that the redox process was an adsorption-controlled and the immobilized alcohol dehydrogenase was stable. It

can be seen that the redox peak currents increased more linearly with the  $v$  in comparison to that of  $v^{1/2}$ .

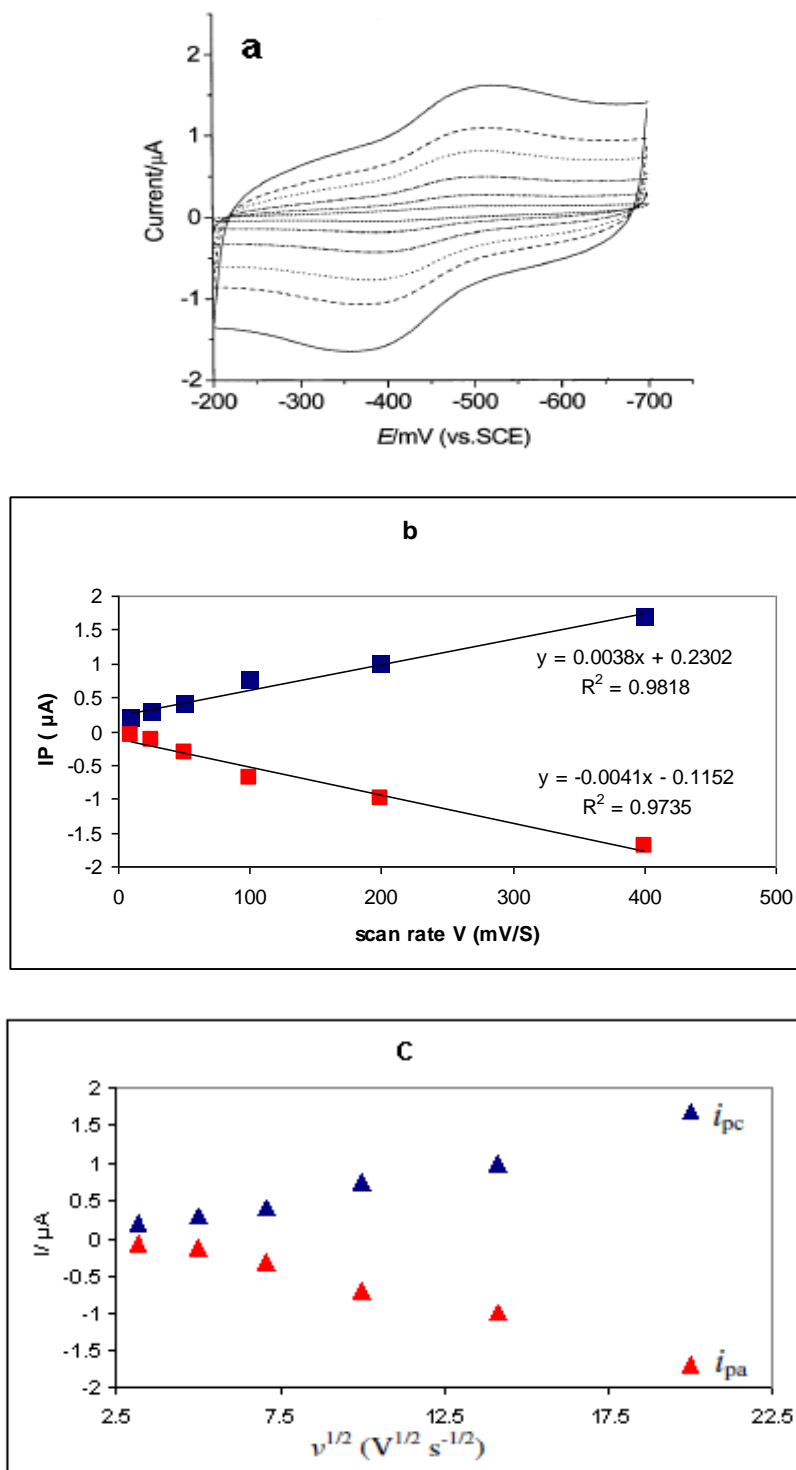


**Figure 4.** (a) CVs of ADH / ZrO<sub>2</sub> Nps/ CPE in PBS 0.1M at various scan rates, from inner to outer; 10, 25, 50, 100, 200 and 400 mV s<sup>-1</sup>, the relationship between the peak currents (*i*<sub>pa</sub>, *i*<sub>pc</sub>) vs., (b) the sweep rates and (c) the square root of sweep rates. Blue lines are redox peaks and red lines are oxidative peaks.

All these results indicated that the ADH immobilized into ZrO<sub>2</sub> Nps/ CPE underwent a surface controlled and quasi-reversible electrochemical reaction process. When the peak-to-peak separation ( $\Delta E$ ) was larger than 200 mV, the apparent heterogeneous electron transfer rate constants ( $k_s$ ) would be easily calculated with the help of Laviron's consistent with the reported potential values for redox state in the ADH [30–31]. These results suggested that direct electron transfer of the ADH molecules entrapped in ZrO<sub>2</sub> Nps/ CPE was enhanced. However, there is clearly a systematic deviation from linearity in this data, i.e. low scan rates are always on one side of the line and the high scan rate points are on the other. The anodic and cathodic peak potentials are linearly dependent on the logarithm of the scan rates ( $v$ ) when  $v > 1.0 \text{ V s}^{-1}$ , which was in agreement with the Laviron theory, with slopes of  $-2.3RT/\alpha nF$  and  $2.3RT/(1-\alpha)nF$  for the cathodic and the anodic peak, respectively [32]. So, the charge-transfer coefficient ( $\alpha$ ) was estimated equal to 0.48. (Given  $0.3 < \alpha < 0.7$  in general). Furthermore, the heterogeneous electron transfer rate constant ( $k_s$ ) was estimated according to the following equation [33]:

$$\left[ \log k_s = \alpha \log(1-\alpha) + (1-\alpha) \log \alpha - \log nFv - \frac{RT}{2.3 RT} \frac{\alpha(1-\alpha)nF\Delta E_p}{RT} \right] \quad (1)$$

Here,  $n$  is the number of transferred electrons at the rate of determining reaction and  $R$ ,  $T$  and  $F$  symbols having their conventional meanings.  $\Delta E_p$  is the peak potential separation. The  $\Delta E_p$  was equal to 40, 70, -95, -120 and -180 mV at 10, 25, 50, 100, 200 and 400  $\text{mV s}^{-1}$ , respectively, giving an average heterogeneous transfer rate constant ( $k_s$ ) value of  $2.3 \text{ s}^{-1}$ .

#### 3.4. Design Alcohol biosensor for determination of ethanol

Electrocatalytic oxidation of ethanol in acidic [34-35], alkaline [36] or near neutral [37] pH has been studied widely using voltammetry technique for fuel cells, electrochemical sensors, and biosensors applications. However, to achieve rapid response and wide linear range of ethanol detection at the modified electrode surface, voltammetry technique can be more effective to probe the ethanol electrocatalytic oxidation reaction. The performances of the disposable biosensors were tested by applying it to the determination of the ethanol concentration of different beverages. In this study, the concentration of ethanol was determined by using the standard addition method due to elimination of matrix effects. Upon addition of ethanol to 0.1M pH 7.0 PBS, the cyclic voltammogram of the ADH / ZrO<sub>2</sub> Nps/ CPE for the direct electron transfer of ADH changed dramatically with an increase of reduction peak current and a decrease of oxidation peak current (Fig. 5(a)), while the change of cyclic voltammogram of bare or ZrO<sub>2</sub> Nps/ CPE was negligible (not shown), displaying an obvious electrocatalytic behavior of the ADH to the reduction of ethanol. The Calibration curve (Figure 5(b)) shows the linear dependence of the cathodic peak current on the ethanol concentration in the range of 1 to 26 mM. In Figure 5(b), at higher concentration of ethanol, the cathodic peak current decreased and remains constant. Upon addition of an aliquot of ethanol to the buffer solution, the reduction current increased steeply to reach a stable value (Figure 5(b)). This implies electrocatalytic property of electrode. As can be observed, the sensor response shows good linearity in this range. The correlation

factor,  $R^2$  was found to be 0.9984. Thus, this experiment has introduced a new biosensor for the sensitive determination of ethanol. The detection limit of this method was significantly lower than those of other methods for alcohol determination and it was sufficient to monitor ethanol in clinical applications with reference to urine or blood; also this biosensor can be use in industrial activities. The reaction 2 corresponded to reduction and oxidation peaks:

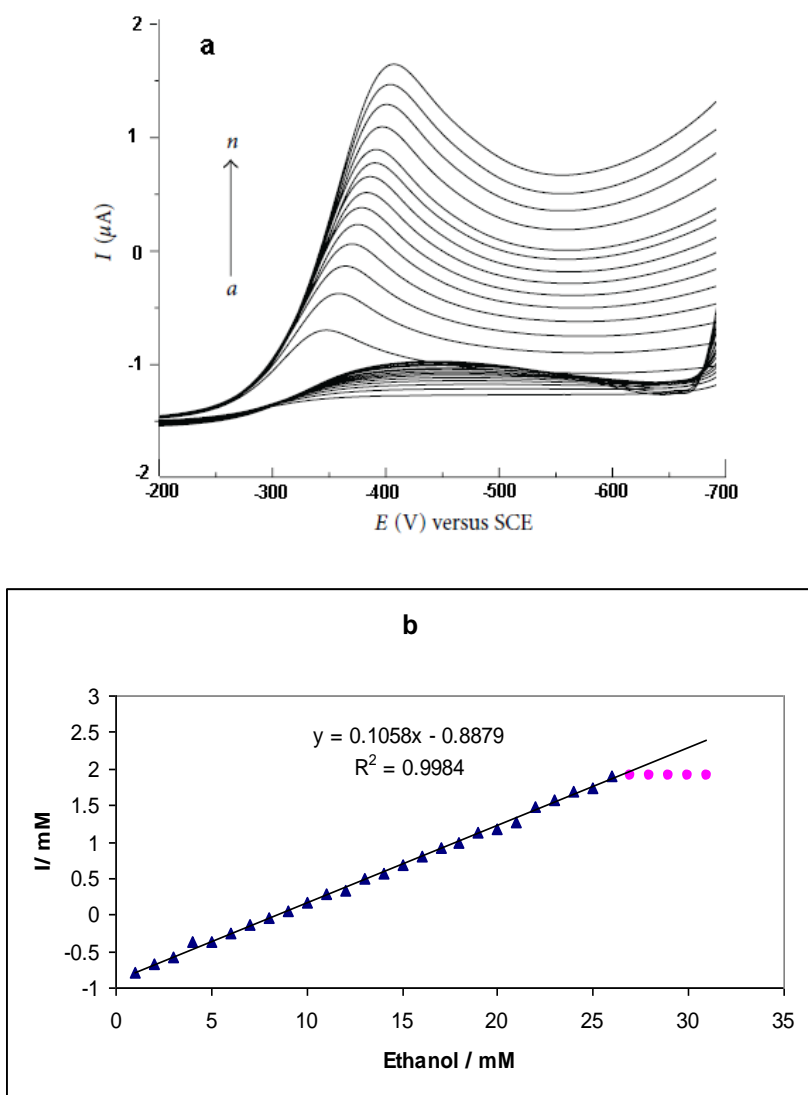
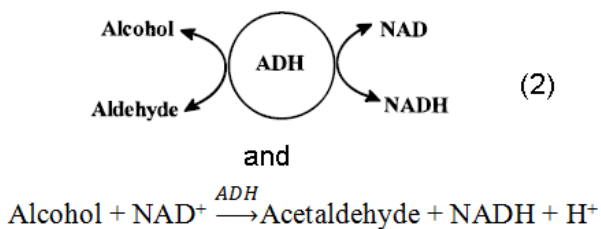


**Figure 5.** (a) Cyclic voltammograms obtained at an ADH /  $\text{ZrO}_2$  Nps/ CPE in 0.1M phosphate buffer solution (pH 7.0) for different concentrations (1 to 26 mM) of ethanol and (b) the relationship between cathodic peak current of ADH and different concentrations of ethanol (scan rate:  $50 \text{ mVs}^{-1}$ ).



### 3.5. Alcohol biosensor lifetime

The operational stability was examined by measuring the response to 1 mM ethanol. The sensors were stored in 0.1 M PBS (pH 7.0) at 7 Celsius degree for 21 days, while measurements were conducted every 2 days during the first week and then once a week subsequently. The response did not change significantly.

## 4. CONCLUSION

In this research, a novel biosensor for detect ethanol has been developed. Direct electron transfer of the ADH immobilized into the ZrO<sub>2</sub> Nps/ CPE was greatly facilitated. The established biosensor exhibited fast response, high sensitivity, good reproducibility and stability. The fast electron transfer rate and excellent catalytic ability to the reduction of ethanol also show that the ADH retains its bioactivity well. The excellent performances may be ascribed to the unique properties conductivity and biocompatibility of ZrO<sub>2</sub> nanoparticles and these nanoparticles were very useful for the future development of the new nanodevices such as electrochemical biosensors.

## ACKNOWLEDGEMENT

Department of Biology, Payame Noor University .I.R, of IRAN and Kermanshah University of medicine, Kermanshah, Iran supported this research work.

## References

1. A.K.H. Cheng, D. Sen, H. Yu, *Bioelectrochemistry*, 77 (2009) 1.
2. M.K. Bessenhirtz, F.W. Scheller, W.F.M. Stocklein, D.G. Kurth, H. Mhwald, F. Lisdat, *Angew. Chem. Int. Ed.* 43 (2004) 4357.
3. Y. Xiao, F. Patolsky, E. Katz, J.F. Hainfeld, I. Willner, *Science.*, 299 (2003) 1877.
4. J. Lagueze, K.E. Kirat, S. Morandat, *Colloids Surf.* 79 (2010) 33.
5. O.A. Sadik, S.K. Mwilu, A. Aluoch, *Electrochim. Acta.*, 55 (2010) 4287.
6. A.P.F. Turner, *Science.*, 290 (2000) 1315.
7. Arnold, M. A., and M. E. Meyerhoff, *Rev. Anal. Chem.*, 20 (1988) 149.
8. Mendelson, Y., "Optical sensors." In J. G. Webster (ed.), *Encyclopedia of Medical Devices and Instrumentation.*, 5 (2006) 160.
9. Andolfi, L.; S. Ismail, Z. A. Ahmad, A. Berenov, and Z. Lockman, *Corrosion Science*, 53 (2011) 1156.
10. Luong, J.H.T., Groom, C.A. and Male, K.B. *Biosensors and Bioelectronics* 6 (1991) 547.
11. Wang, J., Pamidi, P.V.A. and Jiang, M. *Anal. Chim. Acta* 360 (1998) 171.
12. Zhang, J., Li, B., Wang, Z., Cheng, G. and Dong, S. *Anal. Chim. Acta* 388 (1999) 71.
13. Munteanu, F.D., Kubota, L.T. and Gorton, L. *J. Electroanal. Chem.* 509 (2001) 2.
14. Bremle, G., Persson, B. and Gorton, L. *Electroanalysis* 3 (1991) 77.
15. Wedge, R., Pemberton, R.M., Hart, J.P. and Luxton, R. *Analysis* 27 (1999) 570.
16. Sandström, K.J.M., Newman, J., Sunesson, A.-L., Levin, J.-O. and Turner, A.P.F. *Sens Actuators B70* (2000) 182.

17. Avramescu, A., Noguer, T., Magearu, V and Marty J-L. *Anal. Chim. Acta* 433 (2001) 81.
18. Sprules, S.D, Hart, J.P, Wring, S.A. and Pittson, R. *Analyst* 119 (1994) 253.
19. Korpan, Y.I., Dzyadevich, S.V., Zharova, V.P. and El'skaya, A.V. *Ukr. Biokhim. Zh.* 66 (1994) 78.
20. Korpan, Y.I., Gonchar, M.V., Soldatkin, A.P., Starodub, N.F., Sandrovski, A.K., Sibirnyi, A.A. and El'skaia, A.V. *Ukr. Biokhim. Zh.* 64 (1992) 96.
21. Rotariu, L., Bala, C. and Magearu, V. *Anal. Chim. Acta* 458 (2002) 215.
22. Rotariu, L., Bala, C. and Magearu, V. *Rev. Roum. Chim.* 45 (2000) 21.
23. Leca, B. and Marty, J. *Biosens. Bioelectron.* 12 (1997) 1083.
24. Xie, X., Subiman, A.A., Guilbault, G.G. and Yang, Z. *Anal. Chim. Acta* 266 (1992) 325.
25. Marko-Varga, G., Johansson, K. and Gorton, L. *J. Chromatogr. A.* 660 (1994) 153.
26. Chung, S.Y., Vercellotti, J.R. and Sanders, T.H. *J. Agr. Food Chem.* 43 (1995) 1545.
27. H. Tsuchiya, J. M. MacAk, L. Taveira, and P. Schmuki, *Chemical Physics Letters*, 410 (2005) 188.
28. H. Fan, L. Yang, W. Hua et al., *Nanotechnology*, 15 (2004) 37.
29. A.J. Bard, L.R. Faulkner, *Electrochemical Methods*, second. ed., *Fundamentals and Applications*, Wiley, NY(2001) 241.
30. D. Britz, *J. Electroanal. Chem.* 88 (1978) 309.
31. A. Salimi, E. Sharifi, A. Noorbakhsh, S. Soltanian, *Biophys. Chem.* 125 (2007) 540.
32. E. Laviron, *J. Electroanal. Chem.*, 100 (1979) 263.
33. E. Laviron, *J. Electroanal. Chem.* 101 (1979) 19.
34. Park, J.K.; Yee, H.J.; Lee, K.S.; Lee, W.Y.; Shin, M.C.; Kim, *Anal. Chim. Acta.*, 390 (1999) 83.
35. Svensson, K.; Bülow, L.; Kriz, D.; Krook, M. *Biosens. Bioelectron.* , 21 (2005) 705.
36. Harmon, B.J.; Patterson, D.H.; Regnier, F.E. *J. Chromatogr.*, 657 (1993) 429.
37. Sanford, C.L.; Mantooth, B.A.; Jones, B.T. *J. Chem. Educ.*, 78 (2001) 1221.